Graphene on metal surfaces and its hydrogen adsorption: A meta-GGA functional study

Mie Andersen, Liv Hornekær, and Bjørk Hammer
Interdisciplinary Nanoscience Center and Department of Physics and Astronomy, Aarhus University, DK-8000 Aarhus C, Denmark
(Received 6 February 2012; published 3 August 2012)

The interaction of graphene with various metal surfaces is investigated using density functional theory and the meta-generalized gradient approximation (MGGA) M06-L functional. We demonstrate that this method is of comparable accuracy to the random-phase approximation (RPA). With M06-L we study large systems inaccessible to RPA with H adsorbed on graphene on a selected strongly (Ni) and a selected weakly (Pt) interacting substrate. Very stable graphane-like clusters, where every other C atom binds to a H atom above and every other to a metal atom below, are found on both substrates. Such graphane-like clusters have been proposed to be responsible for opening a band gap in graphene. On Ni we find that the binding energies of the H clusters are almost constant with the cluster size, whereas on Pt the binding energies increase with the cluster size. Comparing the Perdew-Burke-Ernzerhof and M06-L functionals we demonstrate the importance of accounting for dispersive interactions.

DOI: 10.1103/PhysRevB.86.085405 PACS number(s): 73.22.Pr, 71.15.Mb, 73.20.At

I. INTRODUCTION

Since the first experimental synthesis and characterization of graphene in 2004,[1] this two-dimensional (2D) material has attracted continued interest due to its remarkable structural and electronic properties,[2] such as the linear dispersion in the band structure around the Fermi level and the exceptionally high electron mobility. While the first graphene samples were produced from mechanical exfoliation of graphite, epitaxial growth on metal surfaces has proven a very efficient method for producing large-scale graphene samples.[3] Experiments show that the electronic properties of adsorbed graphene are highly dependent on the underlying metal substrate. On Ni(111) and Co(0001)[4,5] there is a strong hybridization between the carbon p_z orbitals and the metal d states inducing large band gap openings. On Pd(111) and for graphene intercalated with Cu or Ag,[6,7] small band gap openings of ∼0.2–0.3 eV have been observed, whereas on Pt(111) and Au(111),[7–9] the graphene band structure is unperturbed except from a small doping. An understanding of the graphene-metal interaction is very important also for the process of making nanoscale devices with graphene, as these must be connected to metal electrodes.

It remains challenging to describe graphene adsorption on metals with density functional theory (DFT) since many functionals fail in treating dispersive interactions. The local-density approximation (LDA) correctly reproduces the division into strongly and weakly interacting metals.[10] On the other hand, the generalized gradient approximation functionals (GGAs), which for many systems correct for the overbinding of LDA, yield no binding of the graphene sheet.[11] This gives us reason to suspect that the apparent success of LDA is due to a cancellation of errors rather than a correct description of the physics. There have been several attempts to introduce nonlocal dispersive interactions. van der Waals functionals (vdW-DF and vdW-DF2)[12,13] have been applied with varying success.[14,15] The results seem to be highly dependent on the underlying exchange functional, but a good agreement with experiments was found using vdW-DF2 in combination with the C09 exchange functional of Cooper.[16] More recently, a higher-level, but computationally very costly, functional using the random-phase approximation (RPA) was used to study graphene on Ni(111)[17] and graphene on Ni(111), Co(0001), and Cu(111),[18] and it was shown that the bonding in these systems is a delicate balance between covalent and dispersive interactions. Another approach to vdW interactions is given by the empirical dispersion correction scheme of Grimme (DFT-D).[19] This was used with success to describe graphene on Ru(0001).[20]

In this paper we present results obtained using the meta-generalized gradient approximation (MGGA), which, in addition to the electron density and its gradient used in GGAs, also includes the kinetic energy density in the functional expression. The specific MGGA functional used is M06-L,[21] which was constructed by fitting the functional form to a large database of organic and organometallic compounds. The database included also systems with noncovalent interactions such as hydrogen-bonding dimers and π-π stacking complexes. The M06-L functional has been applied to a large number of systems, covering areas such as organic, inorganic, and biological chemistry, catalysis, and kinetics.[22] Studies on systems with noncovalent interactions, e.g., potential-energy surfaces for small peptides containing aromatic residues[23] and binding energies of neutral and charged water clusters,[24] have validated its robustness in treating such systems outside of the fitted database. Furthermore, in a study of several layered structures including graphite, the M06-L functional has proven capable of treating systems with mixed covalent and dispersive interactions.[25]

This paper is organized as follows: The computational details are given in Sec. II. In Sec. III A the interaction between graphene and various metal surfaces is investigated, and the accuracy of the M06-L functional in describing such dispersive interactions is validated. Section III B deals with H adsorption on two selected metal surfaces, Ni(111) and Pt(111), which represent a strongly and a weakly interacting substrate. Finally, the conclusions are summed up in Sec. IV.

II. COMPUTATIONAL DETAILS

The calculations were performed with the real-space projector-augmented wave code GPAW[26,27] using the recently

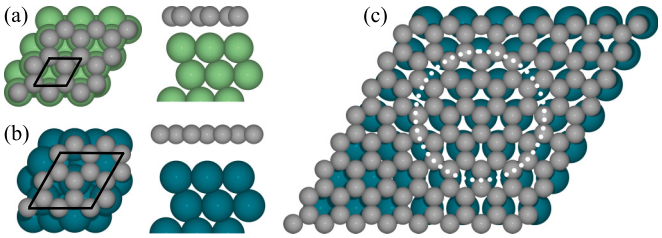

FIG. 1. (Color online) Adsorption geometry for graphene on (a) Ni and Cu(111) and on (b) Pd, Ag, Pt, Au, and Al(111). Top views with unit cell shown in black and side views. The geometry for Co(0001) is similar to (a). (c) Pt-graphene supercell for studying H adsorption (only top Pt layer is shown). H clusters are adsorbed in the region enclosed by the white dotted circle.

implemented[28] M06-L exchange-correlation (XC) functional. For studying the metal-graphene binding we used five-layer metal slabs with graphene adsorbed on one side and a vacuum region of 7.5 Å on each side. Two-dimensional periodic boundary conditions were employed parallel to the slab. The graphene lattice constant was fixed to its optimized value of 2.451 Å, and the metal lattice constants were adapted accordingly. To conform with previous studies we adopted the adsorption geometries from Ref. 10, meaning that Ni, Co, and Cu were treated in (1×1) cells while Pd, Ag, Pt, Au, and Al were treated in $(\sqrt{3} \times \sqrt{3})$ cells [cf. Figs. 1(a) and 1(b)]. For the small and large cells we used k-point samplings of (8×8) and (4×4), respectively. The grid spacing was 0.16 Å. For Ni and Co spin polarization was taken into account. The Fermi level shifts were calculated as the energy difference between the crossing of the two graphene π bands and the Fermi level.

For studying H adsorption on graphene on Ni and on freestanding graphene we expanded the unit cells to (6×6) supercells in order to avoid interactions between H clusters in different periodic images. On Pt we used the (8×8) graphene sheet on the (7×7) Pt slab [Fig. 1(c)], whereby we achieved the same rotation of the graphene sheet relative to the metal substrate as on Ni. Furthermore, we studied an infinite graphane-like structure on Ni and graphane [see Fig. 6] in (1×1) cells. For all cells three-layer metal slabs and a grid spacing of 0.18 Å were sufficient. Otherwise, the computational details were as described for the metal-graphene binding, providing the same or better k-point sampling. The charge transfer upon adsorption of the graphene sheet on the metal surface was calculated from the difference between the charge density in the metal-graphene structure and the charge densities in the isolated metal slab and graphene sheet kept in the exact same positions as in the metal-graphene structure.

III. RESULTS AND DISCUSSION

A. Metal-graphene binding

The binding distances and binding energies are given in Table I along with results from the literature obtained with other XC functionals and available experimental data. On Co and Ni we find two local minima: a chemisorbed minimum with a binding distance around 2.3 Å and a physisorbed minimum with a binding distance around 3.25 Å. On both substrates the local minima are close in energy, with the physisorbed being slightly more favorable. On Ag, Au, Cu, Pt, and Al the binding distances are around 3.4 Å, indicating a physisorbed graphene sheet with mainly dispersive interactions. On Pd the binding is intermediate with a binding distance around 3 Å.

Interestingly, in contrast to the LDA and vdW-DF2^{C09_x} results, we do not find correspondingly higher binding energies for the chemisorbed minima on Ni and Co. This is similar

TABLE I. Equilibrium binding distances d_{eq} (in Å) and binding energies E_b (in meV per carbon atom) for graphene on various metal surfaces along with Fermi-level shifts ΔE_F (in eV) for weakly interacting metals. A negative (positive) ΔE_F indicates n- (p)-type doping. For results given in italic the graphene lattice constant has been adjusted to the optimized metal lattice constant and vice versa for nonitalic results.

	Parameter	Co	Ni	Pd	Cu	Ag	Pt	Au	Al
M06-L	d_{eq}	2.29/3.25[a]; *2.27/3.23*[a]	2.37/3.25[a]; *2.29/3.25*[a]	3.06	3.31; *3.32*	3.37	3.38	3.40	3.53
	E_b	54/58[a]; *82/66*[a]	44/61[a]; *64/64*[a]	79	57; *61*	56	62	54	39
	ΔE_F				−0.07	−0.22	0.31	0.15	−0.31
LDA[b]	d_{eq}	2.05	2.05	2.30	3.26	3.33	3.30	3.31	3.41
	E_b	160	125	84	33	43	38	30	27
vdW-DF[c]	d_{eq}	*3.40*	*3.50*	*3.50*	*3.58*	*3.55*	*3.67*	*3.57*	*3.72*
	E_b	*30*	*37*	*39*	*38*	*33*	*43*	*38*	*35*
vdW-DF2^{C09_x}[d]	d_{eq}		*2.07*	*2.92*	*2.94*	*3.23*	*3.24*	*3.29*	
	E_b		*141*	*72*	*62*	*53*	*68*	*59*	
RPA[e]	d_{eq}	*2.3/3.25*[a]	*2.3/3.25*[a]		*3.25*				
	E_b	*86/74*[a]	*69/77*[a]		*62*				
Experiment	d_{eq}		2.1[f]				3.3[g]		

[a]Two local minima are found.
[b]Reference 10.
[c]Reference 14.
[d]Reference 15.
[e]Reference 18.
[f]Reference 29.
[g]Reference 8.

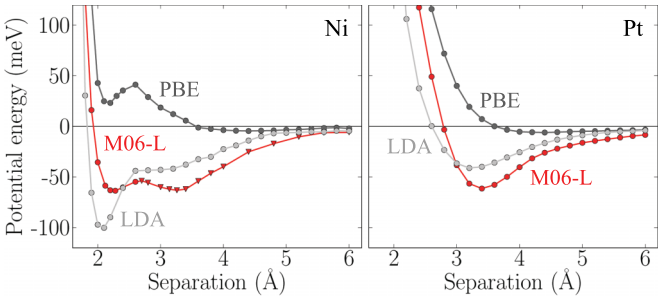

FIG. 2. (Color online) Potential energy per C atom of graphene on Ni and Pt as a function of the graphene-metal separation. For the circular points the GPAW eigenstates were converged to 10^{-7}–10^{-8} eV^2 per valence electron, whereas for the triangular points they were converged to 10^{-2}–10^{-3} eV^2 per valence electron.

to RPA results,[18] where the binding energies for Ni and Co are only slightly higher than for Cu. To allow for a direct comparison we performed the calculations for Ni, Co, and Cu using the geometry from Ref. 18, where the graphene lattice constant is adjusted to the optimized metal lattice constant (results shown in italic in Table I). Stretching the graphene leads to somewhat larger binding energies for the chemisorbed minima on Ni and Co, and overall, we get both binding distances and energies in excellent agreement with the RPA results.

From low-energy electron diffraction (LEED) studies on Ni (Ref. 29) it is known that the graphene lattice constant is stretched to match the Ni lattice constant and that the binding distance (2.1 Å) is characteristic of a chemisorbed state. From our results using this geometry, it is below the limit of accuracy to determine if the chemisorbed or physisorbed state is most favorable. On Co(0001), scanning tunneling microscope (STM) measurements revealed a stretching of the graphene to match the Co lattice as well as a strong electronic coupling between the graphene π states and the Co d states indicative of a chemisorbed graphene sheet.[5] The M06-L results for this geometry show a clear preference of the chemisorbed state (82 vs 66 meV), in agreement with the experimental result.

In Fig. 2 we plot the potential energy per C atom for graphene on Ni and Pt as a function of the graphene-metal separation with the LDA, Perdew-Burke-Ernzerhof (PBE), and M06-L functionals. Relaxation effects were not taken into account since they are very small. On Ni, the M06-L potential energy curve with two equally deep local minima is in excellent agreement with the RPA results. In contrast, LDA overbinds the graphene sheet, whereas PBE yields almost no binding. On Pt, the LDA functional underestimates the binding energy compared to M06-L, whereas PBE again yields almost no binding. RPA results for the Pt-graphene binding are not available; however, the M06-L binding distance of 3.38 Å is in excellent agreement with the experimental result of 3.3 Å.[8] These results underline the ability of the M06-L functional to describe the interaction of graphene with both strongly and weakly interacting substrates.

To further examine the graphene-metal interaction we calculate the band structure along graphene high-symmetry directions in the Brillouin zone (Fig. 3). On Ni a strong

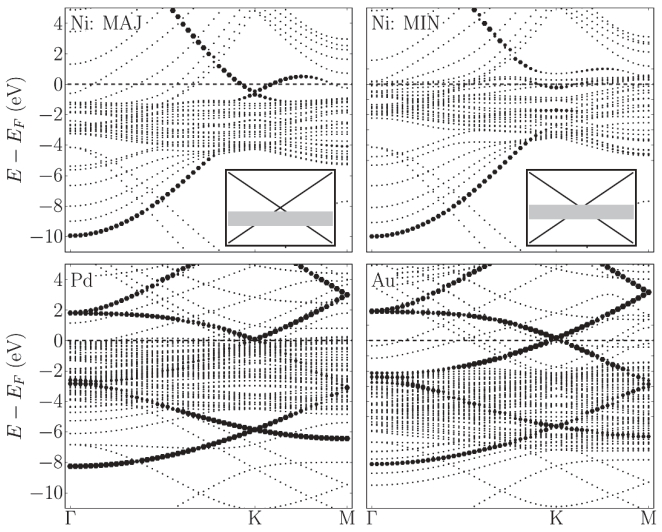

FIG. 3. Band structure of graphene on Ni(111), Pd(111), and Au(111). The size of the markers represents the weight on the carbon p_z orbitals. For graphene on Ni(111) both majority (MAJ) and minority (MIN) spin channels are shown. Insets sketch the positions of the d bands relative to the Dirac cone.

hybridization between the C p_z orbitals and the Ni d states is seen, which disrupts the conical shape of the graphene π bands and induces a band gap opening. This is in good agreement with experiments[4] and LDA, vdW-DF2^{C09_x}, and RPA results. The different band dispersions for majority and minority spins arise from the different positions of the Ni d bands relative to the graphene Dirac cone, as illustrated in the insets. A similar result is obtained for Co (not shown). On Pd the hybridization is less pronounced, resulting only in a smearing of the occupied parts of the graphene π bands. A band gap opening is not observed, in disagreement with the experimental result[6] and the LDA result but in agreement with the vdW-DF2^{C09_x} result. However, it has been argued[15] that this is a result of not using the appropriate moiré superstructure. On Au the graphene band structure is unperturbed around the Fermi level except from a small p-type doping. This is in good agreement with experiments[7] and LDA results, whereas vdW-DF2^{C09_x} yields a small n-type doping instead. Similar results are obtained on Ag, Cu, Pt, and Al (not shown). In Table I the Fermi-level shifts for all weakly interacting metals are summarized.

B. Hydrogen adsorption

H adsorption can be considered a probe of the reactivity of the adsorbed graphene layer, but it also has attracted much attention in the literature in its own right. There are several theoretical predictions[30–32] and a recent experimental verification on Ir-adsorbed graphene[33] that chemical functionalization with H can lead to a band gap opening in graphene. Such a band gap opening is essential to improve the on-off ratio of graphene field-effect transistors.

From the band structure results we expect very different electronic properties and thereby different reactivity of graphene dependent on the metal substrate. As demonstrated so far the M06-L functional is capable of describing the mixed

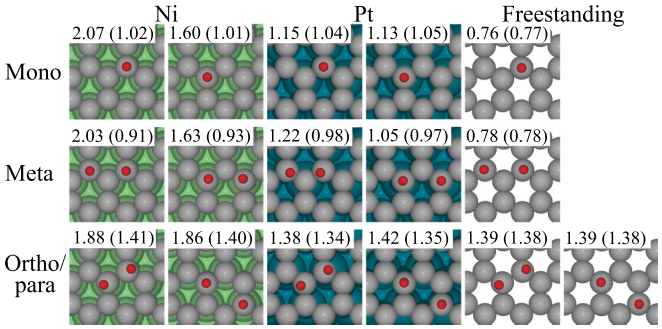

FIG. 4. (Color online) Structures of H monomers, meta dimers, and ortho and para dimers on graphene adsorbed on Ni and Pt and on freestanding graphene. Binding energies per H atom are given in eV using M06-L and PBE (in parentheses).

bonding in these systems to comparable accuracy as RPA, and we expect to maintain this accuracy when the graphene surface is chemically modified. Adsorption processes necessarily involve larger systems, which are inaccessible to RPA. We study the adsorption of H on graphene on a selected strongly (Ni) and a selected weakly (Pt) interacting substrate and compare to freestanding graphene.

Structures and binding energies of the investigated monomers and dimers are shown in Fig. 4. For monomers and meta dimers there are two inequivalent structures with either top or hollow C atoms hydrogenated, whereas only one structure is possible for ortho and para dimers. On Ni, the monomer and meta dimer show a strong preference ($\sim$0.4 eV/H atom) for adsorption on hollow C atoms. This preference can be explained by evaluating the charge transfer which occurs when the graphene sheet is adsorbed on the Ni surface [Fig. 5(b), left]. Charge accumulates between the top C atom and the underlying Ni atom, indicating the formation

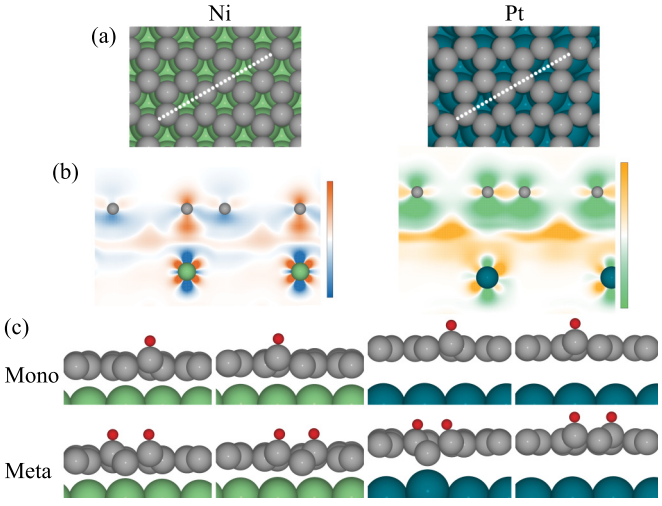

FIG. 5. (Color online) (a) Top views of graphene adsorbed on Ni and Pt. (b) Charge transfer upon adsorption cut along the dotted line in (a). For Ni the color scale ranges from $\Delta\rho = -0.01\ e/\text{Å}^3$ (blue) to $\Delta\rho = 0.01\ e/\text{Å}^3$ (red), whereas for Pt the color scale ranges from $\Delta\rho = -0.001\ e/\text{Å}^3$ (green) to $\Delta\rho = 0.001\ e/\text{Å}^3$ (orange). A negative value indicates a loss of electron density. (c) Side views cut along the dotted line in (a) of the monomers and meta dimers on Ni and Pt.

of a weak covalent bond. The hybridization between the C p_z orbital and the Ni $d_{3z^2-r^2}$ orbital is clearly seen; compare to the band structure of graphene on Ni in Fig. 3. On the other hand, the hollow C atom is depleted of charge, which makes it more reactive towards a H atom. Furthermore, when H atoms are adsorbed on hollow C atoms the covalent bonds between the top C atoms and the Ni atoms can be kept intact or even strengthened, and thereby the H binding energies become very high. The fact that the top C atoms are responsible for the covalent bonding to the substrate is in good agreement with RPA results for the graphene adsorption on Ni.[18]

On Pt, the two monomers have similar binding energies (cf. Fig. 4). Again this can be explained from the charge transfer [Fig. 5(b), right], which does not show any appreciable difference between the top and hollow C atoms. Note that the scale bar for the charge transfer on Pt is a factor of 10 smaller than the scale bar for Ni. For the meta dimer on Pt, hollow sites are favored over top sites by 0.17 eV. The reason for this preference is apparent in the side views in Fig. 5(c) (lower right). With two hydrogenated hollow C atoms it becomes energetically favorable to bend the graphene sheet downwards to make a bond between the unhydrogenated top C atom in the middle of the cluster and the underlying Pt atom.

The ortho and para dimers on Pt have similar binding energies as the corresponding clusters on freestanding graphene (cf. Fig. 4). This is in contrast to the monomers and meta dimers, which are stabilized on metal-adsorbed graphene by $\sim$0.38 and $\sim$0.27 eV/H atom, respectively (ignoring any extra stabilization from bonding to the substrate). The difference between these structures is that monomers and meta dimers result in an uneven hydrogenation of the two graphene sublattices, whereas they are evenly hydrogenated for ortho and para dimers. On freestanding graphene it has previously been shown[34–37] that the formation of monomers and meta dimers yields unpaired electrons, which lead to a ferromagnetic ground state. For monomers and meta dimers on Pt-adsorbed graphene a spin polarized calculation does not reveal any unpaired electrons. We attribute this to the charge transfer from the substrate. This is in good agreement with a recent investigation on the effect of charge doping on the monomer on freestanding graphene,[38] where similar stabilization energies and a decreasing energy splitting between the spin-up and spin-down states in the electronic density of states was found. On Ni, the binding energies of the ortho and para dimers are dominated by covalent bonding to the substrate, as evidenced by the $\sim$0.5 eV/H atom stronger bonding.

The hollow monomer and meta dimer can be considered small graphane-like clusters, where every other C atom binds to a H atom above and every other to a metal atom below. Such graphane-like clusters were proposed in recent studies of H adsorption on graphene on Ir, Pt, and Ni.[33,39] We pursue this trend and investigate larger graphane-like clusters on Ni and Pt and the infinite graphane-like structure on Ni and compare to a finite-size graphane-like cluster on freestanding graphene and graphane. The size of graphane-like clusters is limited on Pt due to the lattice mismatch, as indicated with the dotted circle in Fig. 1(c).

The structures and binding energies of the investigated larger graphane-like clusters are shown in Fig. 6. For large (Pt) or infinite (Ni) clusters the binding energies are similar,

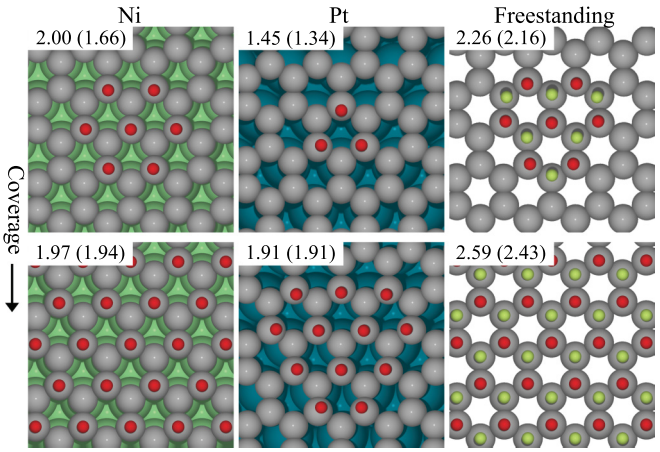

FIG. 6. (Color online) Structures of larger graphane-like H clusters on graphene on Ni and Pt and on freestanding graphene at various coverages. On freestanding graphene H atoms attached from below (above) are shown in yellow (red). Binding energies per H atom are given in eV using M06-L and PBE (in parentheses).

around 1.9 eV. On freestanding graphene both the finite graphane-like cluster and graphane have considerably higher binding energies. Thus, it is more favorable for the H atoms to adsorb in a structure with H atoms bonding from both sides of the graphene sheet instead of bonding to the metal substrate on one side and to H from the other.

Fig. 7(a) summarizes the evolution in H binding energies as a function of coverage for the graphane-like clusters. On Ni, the binding energies are almost constant with the cluster size since graphane-like clusters can be formed already at the lowest coverage. On Pt, H monomers and dimers are not very stable. Rather, the H binding energy increases with cluster size, rendering even ortho and para dimers on Pt much less stable than, e.g., 12 H graphane-like clusters. Thus, these dimers are expected to form only at low coverages or on the region of the Pt-graphene unit cell where all C atoms are found on hollow sites [lower left corner of unit cell in Fig. 1(c)]. We propose that the close proximity of graphene to Ni helps stabilize small H clusters since metal-C bonds can form easily, while the larger graphene-metal separation on Pt introduces a deformation cost which is best overcome by large H clusters. Evidence for this is given in Figs. 7(b) and 7(c) (top structures), where side views of the investigated graphane-like clusters are shown. The deformations are small over Ni [Fig. 7(b)] but more sizable over Pt [Fig. 7(c)].

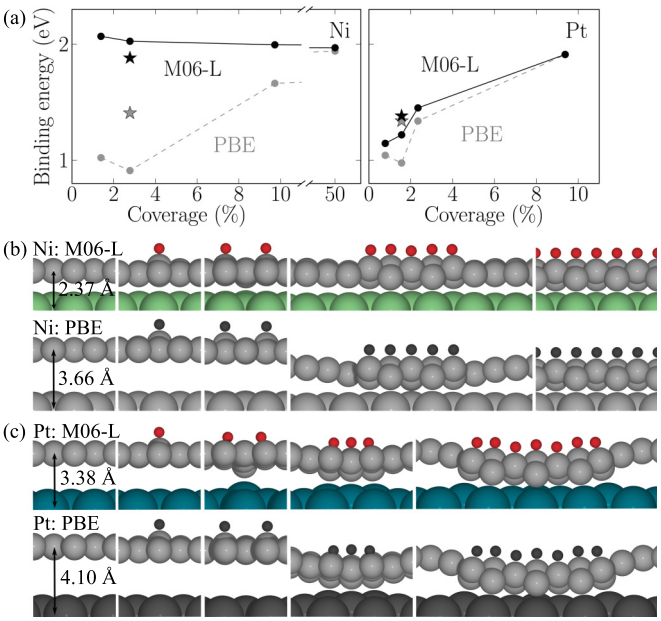

FIG. 7. (Color online) (a) Binding energies per H atom as a function of coverage for graphane-like H clusters (connected dots) and ortho dimers (stars) on graphene adsorbed on Ni (left) and on Pt (right). The two series shown are calculated with M06-L (black line) and PBE (dashed gray line). Side views of graphane-like H clusters on (b) Ni and on (c) Pt calculated with M06-L (color) and PBE (gray scale).

To investigate the importance of dispersive interactions, we repeated some of the H cluster calculations using the PBE functional,[40] which fails to describe dispersive interactions and yields a repulsive graphene-metal interaction (see Fig. 2). The resulting larger graphene-metal separation in PBE, which is apparent in Figs. 7(b) and 7(c) (bottom structures), acts as a hindrance to the formation of C-Ni or C-Pt bonds, whereby H monomers and dimers become less stable. The effect is so pronounced that with PBE, the H binding energies reverse their trend for Ni to increase with cluster size, as marked with gray symbols and dashed lines in Fig. 7(a). On Pt the differences are only significant at low coverages. Using M06-L, two H atoms are needed in the cluster to achieve a back bonding to the substrate, whereas with PBE three H atoms are needed.

IV. CONCLUSIONS

In conclusion we have shown that the M06-L functional provides an accurate description of the graphene-metal interaction, yet at a moderate computational cost. Our results are in good agreement with available experimental data and with results obtained from the much more computationally costly RPA functional. We studied H adsorption on graphene on a strongly (Ni) and a weakly (Pt) interacting substrate. On Ni, the binding energies are almost constant with the cluster size, whereas on Pt the binding energies increase with the cluster size. Large graphane-like clusters have similar binding energies on both substrates. Comparing results obtained with the M06-L and PBE functionals shows the importance of using a functional that provides an accurate description of the graphene-metal interaction. The error made using PBE instead of M06-L is largest at low H coverages and for the strongly interacting substrate (Ni).

ACKNOWLEDGMENTS

Support from the Danish Research Councils, the Lundbeck Foundation, and the Danish Center for Scientific Computing is acknowledged.

[1] K. S. Novoselov, A. K. Geim, S. V. Morozov, D. Jiang, Y. Zhang, S. V. Dubonos, I. V. Grigorieva, and A. A. Firsov, Science **306**, 666 (2004).
[2] K. S. Novoselov, A. K. Geim, S. V. Morozov, D. Jiang, M. I. Katsnelson, I. V. Grigorieva, S. V. Dubonos, and A. A. Firsov, Nature (London) **438**, 197 (2005).
[3] S. Bae, H. Kim, Y. Lee, X. Xu, J.-S. Park, Y. Zheng, J. Balakrishnan, T. Lei, H. R. Kim, Y. I. Song, Y.-J. Kim, K. S. Kim, B. Ozyilmaz, J.-H. Ahn, B. H. Hong, and S. Iijima, Nat. Nanotechnol. **5**, 574 (2010).
[4] A. Varykhalov, J. Sánchez-Barriga, A. M. Shikin, C. Biswas, E. Vescovo, A. Rybkin, D. Marchenko, and O. Rader, Phys. Rev. Lett. **101**, 157601 (2008).
[5] D. Eom, D. Prezzi, K. T. Rim, H. Zhou, M. Lefenfeld, S. Xiao, C. Nuckolls, M. S. Hybertsen, T. F. Heinz, and G. W. Flynn, Nano Lett. **9**, 2844 (2009).
[6] S.-Y. Kwon, C. V. Ciobanu, V. Petrova, V. B. Shenoy, J. Bareno, V. Gambin, I. Petrov, and S. Kodambaka, Nano Lett. **9**, 3985 (2009).
[7] A. Varykhalov, M. R. Scholz, T. K. Kim, and O. Rader, Phys. Rev. B **82**, 121101 (2010).
[8] P. Sutter, J. T. Sadowski, and E. Sutter, Phys. Rev. B **80**, 245411 (2009).
[9] Z. Klusek, P. Dabrowski, P. Kowalczyk, W. Kozlowski, W. Olejniczak, P. Blake, M. Szybowicz, and T. Runka, Appl. Phys. Lett. **95**, 113114 (2009).
[10] G. Giovannetti, P. A. Khomyakov, G. Brocks, V. M. Karpan, J. van den Brink, and P. J. Kelly, Phys. Rev. Lett. **101**, 026803 (2008).
[11] M. Fuentes-Cabrera, M. I. Baskes, A. V. Melechko, and M. L. Simpson, Phys. Rev. B **77**, 035405 (2008).
[12] M. Dion, H. Rydberg, E. Schroder, D. C. Langreth, and B. I. Lundqvist, Phys. Rev. Lett. **92**, 246401 (2004).
[13] K. Lee, E. D. Murray, L. Kong, B. I. Lundqvist, and D. C. Langreth, Phys. Rev. B **82**, 081101 (2010).
[14] M. Vanin, J. J. Mortensen, A. K. Kelkkanen, J. M. Garcia-Lastra, K. S. Thygesen, and K. W. Jacobsen, Phys. Rev. B **81**, 081408 (2010).
[15] I. Hamada and M. Otani, Phys. Rev. B **82**, 153412 (2010).
[16] V. R. Cooper, Phys. Rev. B **81**, 161104 (2010).
[17] F. Mittendorfer, A. Garhofer, J. Redinger, J. Klimes, J. Harl, and G. Kresse, Phys. Rev. B **84**, 201401 (2011).
[18] T. Olsen, J. Yan, J. J. Mortensen, and K. S. Thygesen, Phys. Rev. Lett. **107**, 156401 (2011).
[19] S. Grimme, J. Comput. Chem. **27**, 1787 (2006).
[20] D. Stradi, S. Barja, C. Diaz, M. Garnica, B. Borca, J. J. Hinarejos, D. Sánchez-Portal, M. Alcami, A. Arnau, A. L. Vázquez de Parga, R. Miranda, and F. Martin, Phys. Rev. Lett. **106**, 186102 (2011).
[21] Y. Zhao and D. G. Truhlar, J. Chem. Phys. **125**, 194101 (2006).
[22] Y. Zhao and D. G. Truhlar, Chem. Phys. Lett. **502**, 1 (2011).
[23] J. Cao and T. van Mourik, Chem. Phys. Lett. **485**, 40 (2010).
[24] V. S. Bryantsev, M. S. Diallo, A. C. T. van Duin, and W. A. Goddard, J. Chem. Theory Comput. **5**, 1016 (2009).
[25] G. K. H. Madsen, L. Ferrighi, and B. Hammer, J. Phys. Chem. Lett. **1**, 515 (2009).
[26] J. Enkovaara, C. Rostgaard, J. J. Mortensen, J. Chen, M. Dułak, L. Ferrighi, J. Gavnholt, C. Glinsvad, V. Haikola, H. A. Hansen, H. H. Kristoffersen, M. Kuisma, A. H. Larsen, L. Lehtovaara, M. Ljungberg, O. Lopez-Acevedo, P. G. Moses, J. Ojanen, T. Olsen, V. Petzold, N. A. Romero, J. Stausholm-Møller, M. Strange, G. A. Tritsaris, M. Vanin, M. Walter, B. Hammer, H. Häkkinen, G. K. H. Madsen, R. M. Nieminen, J. K. Nørskov, M. Puska, T. T. Rantala, J. Schiøtz, K. S. Thygesen, and K. W. Jacobsen, J. Phys. Condens. Matter **22**, 253202 (2010).
[27] S. R. Bahn and K. W. Jacobsen, Comput. Sci. Eng. **4**, 56 (2002).
[28] L. Ferrighi, G. K. H. Madsen, and B. Hammer, J. Chem. Phys. **135**, 084704 (2011).
[29] Y. Gamo, A. Nagashima, M. Wakabayashi, M. Terai, and C. Oshima, Surf. Sci. **374**, 61 (1997).
[30] E. J. Duplock, M. Scheffler, and P. J. D. Lindan, Phys. Rev. Lett. **92**, 225502 (2004).
[31] T. G. Pedersen, C. Flindt, J. Pedersen, N. A. Mortensen, A. P. Jauho, and K. Pedersen, Phys. Rev. Lett. **100**, 136804 (2008).
[32] L. A. Chernozatonskii and P. B. Sorokin, J. Phys. Chem. C **114**, 3225 (2010).
[33] R. Balog, B. Jørgensen, L. Nilsson, M. Andersen, E. Rienks, M. Bianchi, M. Fanetti, E. Lægsgaard, A. Baraldi, S. Lizzit, Z. Sljivancanin, F. Besenbacher, B. Hammer, T. G. Pedersen, P. Hofmann, and L. Hornekær, Nat. Mater. **9**, 315 (2010).
[34] D. W. Boukhvalov, M. I. Katsnelson, and A. I. Lichtenstein, Phys. Rev. B **77**, 035427 (2008).
[35] Y. Ferro, D. Teillet-Billy, N. Rougeau, V. Sidis, S. Morisset, and A. Allouche, Phys. Rev. B **78**, 085417 (2008).
[36] S. Casolo, O. M. Løvvik, R. Martinazzo, and G. F. Tantardini, J. Chem. Phys. **130**, 054704 (2009).
[37] Z. Šljivančanin, E. Rauls, L. Hornekær, W. Xu, F. Besenbacher, and B. Hammer, J. Chem. Phys. **131**, 084706 (2009).
[38] L. F. Huang, M. Y. Ni, G. R. Zhang, W. H. Zhou, Y. G. Li, X. H. Zheng, and Z. Zeng, J. Chem. Phys. **135**, 064705 (2011).
[39] M. L. Ng, R. Balog, L. Hornekær, A. B. Preobrajenski, N. A. Vinogradov, N. Mårtensson, and K. Schulte, J. Phys. Chem. C **114**, 18559 (2010).
[40] J. P. Perdew, K. Burke, and M. Ernzerhof, Phys. Rev. Lett. **77**, 3865 (1996).